Cell, Vol. 104, 43–56, January 12, 2001, Copyright ©2001 by Cell Press

CED-1 Is a Transmembrane Receptor that Mediates Cell Corpse Engulfment in *C. elegans*

Zheng Zhou, Erika Hartwieg, and H. Robert Horvitz*
Howard Hughes Medical Institute
Department of Biology
Building 68, Room 425
Massachusetts Institute of Technology
77 Massachusetts Avenue
Cambridge, Massachusetts 02139

Summary

We cloned the *C. elegans* gene *ced-1,* which is required for the engulfment of cells undergoing programmed cell death. *ced-1* encodes a transmembrane protein similar to human SREC (*S*cavenger *R*eceptor from *E*ndothelial *C*ells). We showed that *ced-1* is expressed in and functions in engulfing cells. The CED-1 protein localizes to cell membranes and clusters around neighboring cell corpses. CED-1 failed to cluster around cell corpses in mutants defective in the engulfment gene *ced-7*. Motifs in the intracellular domain of CED-1 known to interact with PTB and SH2 domains were necessary for engulfment but not for clustering. Our results indicate that CED-1 is a cell surface phagocytic receptor that recognizes cell corpses. We suggest that the ABC transporter CED-7 promotes cell corpse recognition by CED-1, possibly by exposing a phospholipid ligand on the surfaces of cell corpses.

Introduction

Programmed cell death (apoptosis) plays an important role in animal development and homeostasis (reviewed by Vaux and Korsmeyer, 1999). One prominent feature shared by all apoptotic deaths is their swift engulfment and digestion by other cells via phagocytosis (Wyllie et al., 1980). This process eliminates unwanted cells before they can release potentially harmful contents and is important for immunological tolerance, suppression of the inflammatory response, and tissue remodeling (Savill et al., 1993).

An engulfing cell recognizes, binds, and internalizes a dying cell, thereby generating a phagosome (Wyllie et al., 1980). The most extensively studied change occurring on the surfaces of apoptotic cells is the exposure of phosphatidylserine (PS), which is associated with loss of phospholipid asymmetry (reviewed by Fadok et al., 1998). Changes of cell surface carbohydrates and charge may also result in distinct features of apoptotic cells recognizable by phagocytes (Savill et al., 1993). Based mostly upon in vitro analyses, a number of mammalian receptors have been suggested to mediate the phagocytosis of apoptotic cells by macrophages and other cell types; these receptors include the *p*hosphatidyl*s*erine *r*eceptor (PSR) (Fadok et al., 2000), integrins, CD14, complement receptors, and several classes of macrophage scavenger receptors (reviewed by Giles et al., 2000). These receptors may function in redundant pathways since inactivation of any single receptor only partially impairs engulfment activity (reviewed by Platt et al., 1998). In *Drosophila melanogaster, croquemort*, a member of the scavenger receptor family, is required for the engulfment of apoptotic corpses by macrophages (Franc et al., 1999).

During the development of a *Caenorhabditis elegans* hermaphrodite, 131 somatic cells and approximately 300 germ cells undergo programmed cell death; these dying cells are rapidly engulfed by neighboring cells (Sulston and Horvitz, 1977; Sulston et al., 1983; Gumienny et al., 1999). Cell corpses are distinguishable with Nomarski differential interference contrast optics by their highly refractile, button-like appearance (Sulston and Horvitz, 1977). Electron microscopy established that engulfing cells extend pseudopodia around cell corpses (Robertson and Thomson, 1982), and engulfed corpses are found within phagosomes inside engulfing cells (Gumienny et al., 1999; also see below), suggesting that the engulfment process in *C. elegans* is similar to that in mammals. However, unlike mammals or *Drosophila*, *C. elegans* does not have macrophage-like mobile phagocytes; rather, cell corpses are engulfed by neighboring cells. Cell types that can function as engulfing cells include hypodermal cells, gonadal sheath cells, pharyngeal muscle cells, and intestinal cells (Robertson and Thomson, 1982; Sulston et al., 1983; Gumienny et al., 1999).

Recessive alleles of six genes, *ced-1*, *ced-2*, *ced-5*, *ced-6*, *ced-7*, and *ced-10*, were isolated in genetic screens for mutants containing persistent cell corpses, and electron-microscopic examinations demonstrated that corpses remain unengulfed in these mutants (Hedgecock et al., 1983; Ellis et al., 1991). Genetic analysis suggests that these genes belong to two functional groups, *ced-1*, *ced-6*, *ced-7*, and *ced-2*, *ced-5*, *ced-10*; single or double mutants within the same group display relatively weak engulfment defects, whereas double mutants between the two groups display stronger defects (Ellis et al., 1991). These results suggest that engulfment in *C. elegans*, as in mammals, involves partially redundant pathways.

ced-2, *ced-5*, and *ced-10* encode homologs of mammalian CrkII, DOCK180, and Rac GTPase, respectively, essential components of intracellular signal transduction pathways that lead to cytoskeletal reorganization during both the engulfment of cell corpses and cell migration; these three genes all act in engulfing cells (Wu and Horvitz, 1998b; Reddien and Horvitz, 2000). The roles of CED-6 and CED-7 are less clear. *ced-6,* which acts in engulfing cells and encodes a protein containing a phosphotyrosine binding (PTB) domain, is similar to the mammalian adaptor proteins Shc, Numb, and Dab (Liu and Hengartner, 1998). *ced-7* encodes a protein similar to ABC (*A*TP *B*inding *C*assette) transporters and

*To whom correspondence should be addressed (e-mail: horvitz@mit.edu).

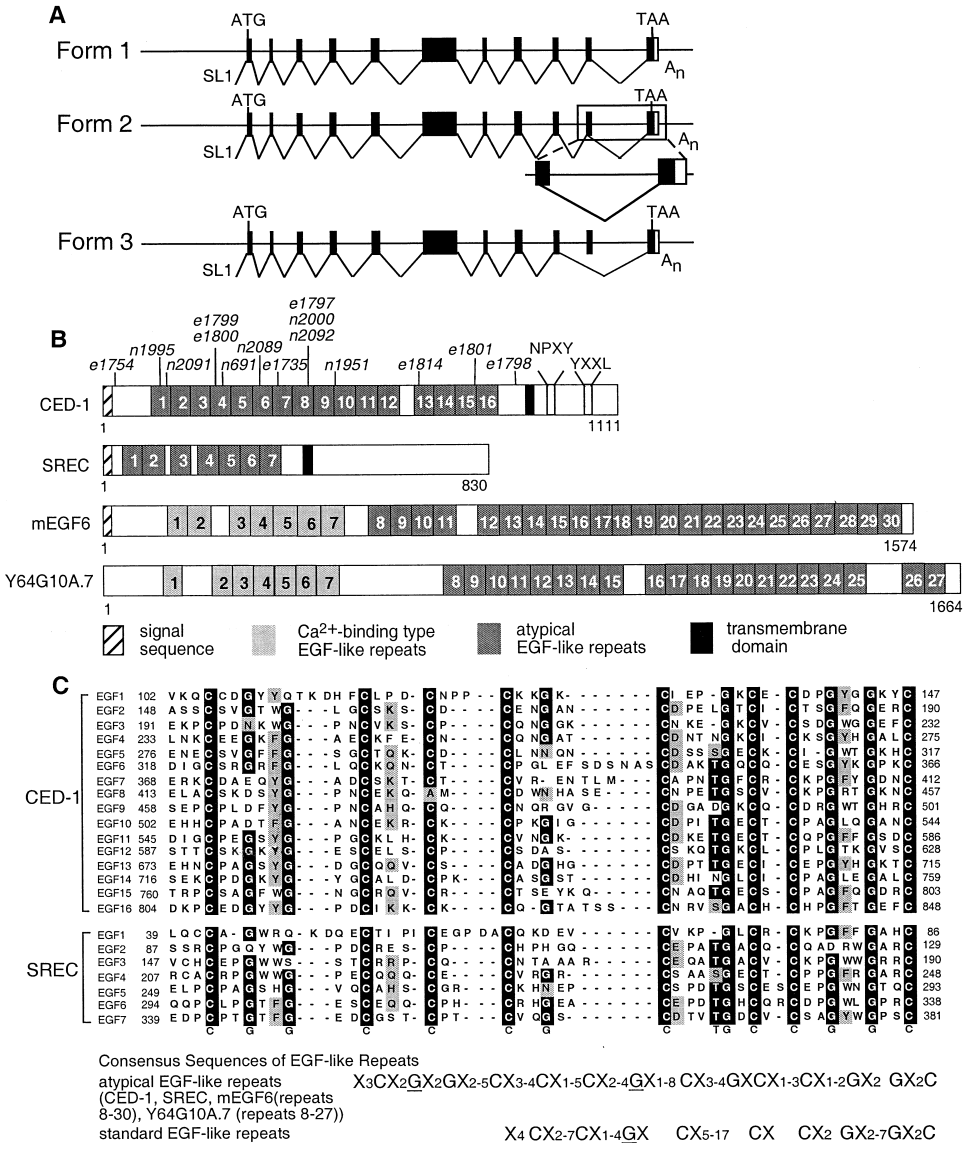

Figure 1. *ced-1* Gene and Protein Structure and Alignments of the EGF-Like Repeats

(A) The structure of *ced-1* as deduced from genomic and cDNA sequences. The longest and most prevalent splice form (Form 1) and two alternative splice forms (Forms 2 and 3) are shown. Solid boxes indicate coding sequences, open boxes indicate noncoding sequences and lines between the solid boxes represent introns. The *trans* spliced leader SL1 is indicated.

(B) Domain structures of CED-1 and related proteins. The locations of the *ced-1* mutations are indicated. Besides the atypical type of EGF-like repeats (gray boxes) shared by all four proteins, mEGF6 and Y64G10A.7 also contain seven copies of a Ca^{2+} binding type of EGF-like repeat (pale gray boxes).

(C) Alignment of the atypical EGF-like repeats in CED-1 and SREC and a comparison to the standard EGF-like repeats. X: any residue. The consensus sequences of Y64G10A.7, mEGF6, and the standard EGF-like repeats are derived from our alignments, Nakayama et al. (1998), and Campbell and Bork (1993), respectively. The glycine residues less than 80% conserved are underlined in the consensus sequences.

appears to function in both dying and engulfing cells (Wu and Horvitz, 1998a). The substrate of CED-7 is unknown.

To understand the role of *ced-1* in the engulfment process and to investigate the signaling pathway controlled by the *ced-1, ced-6, ced-7* group, we cloned and molecularly characterized *ced-1*.

Results

Cloning of *ced-1*

We cloned a 22 kb genomic DNA fragment that rescued the engulfment defect of *ced-1* mutants (see Supplementary Material at *Cell* website http://www.cell.com/cgi/content/full/104/1/43/DC1). This fragment contains a single predicted gene (*C. elegans* Sequencing Consortium, 1998). We then obtained a 3.7 kb *ced-1* cDNA from a *C. elegans* embryonic cDNA library (see Supplementary Material). This cDNA encodes an open reading frame of 1111 amino acids and is likely to be full length as judged by three criteria: its size matches that of the longest corresponding transcript detected on a Northern blot (see Supplementary Material Figure S1C); it contains the last seven nucleotides of the SL1 *trans*-spliced leader sequence (Krause and Hirsh, 1987)

at its 5′ end and a poly(A) tail at its 3′ end (Figure 1A); and expression of this cDNA under the control of *C. elegans* heat shock promoters, which are ubiquitiously expressed in somatic cells upon heat shock treatment (Stringham et al., 1992), fully rescued the *ced-1* mutant phenotype (data not shown). *ced-1* consists of 11 exons (Figure 1A). We also identified two additional alternatively spliced forms of *ced-1* cDNA. An alternative splice-donor site in the middle of exon 10 results in the removal of amino acid residues 1042 to 1082 (Form 2). Another form (Form 3) skips exon 10 entirely, eliminating residues 1017 to 1082 (Figure 1A and see Supplementary Material). Northern analysis indicated that *ced-1* expression is stronger in embryos than in a mixed-staged population (see Supplementary Material Figure S1C).

ced-1 Encodes a Transmembrane Protein that Contains Multiple EGF-like Repeats and Is Similar to Human SREC

The predicted CED-1 protein (Figure 1B) appears to be a transmembrane protein with an amino-terminal extracellular domain of 888 amino acids, a single transmembrane domain of 22 amino acids (Kyte and Doolittle, 1982), and a carboxy-terminal intracellular domain of 181 amino acids. Residues 1 to 20 are predicted to be a signal sequence (Stryer, 1988). The extracellular domain contains 16 motifs that are very similar to each other and to an EGF-like repeat (Figures 1B and 1C). The EGF-like repeat, a cysteine-rich motif located in the extracellular domains of many proteins as tandem repeats, functions in adhesive or ligand receptor interactions (Campbell and Bork, 1993).

CED-1 is most similar to human SREC (*S*cavenger *R*eceptor from *E*ndothelial *C*ells) (Adachi et al., 1997), rat mEGF6 (Nakayama et al., 1998), and a *C. elegans* predicted open reading frame Y64G10A.7 (*C. elegans* Sequencing Consortium, 1998) (Figures 1B and 2). Overall, CED-1 is 38% identical to Y64G10A.7, 31% identical to mEGF6, and 24% identical to SREC. All four proteins contain multiple copies of an atypical type of EGF-like repeat first identified by Nakayama et al. (1998) in mEGF6. This repeat consists of 40 to 45 amino acids, including eight conserved cysteines and four conserved glycines (Figure 1C), and is distinguishable from the standard EGF-like repeat, which contains only six conserved cysteine residues in a region of the same length, and from the laminin type of EGF-like repeat, which includes eight conserved cysteine residues but over a larger (~60 amino acid) region (Campbell and Bork, 1993). This distinct consensus sequence suggests that CED-1, Y64G10A.7, mEGF6, and SREC form a subfamily within the EGF-like repeat-containing protein family. The intracellular domain of CED-1 does not display similarity to any known protein in available databases. This domain contains multiple tyrosine, serine, and threonine residues that are potential phosphorylation sites for protein kinases. It has an NPXY (Asn-Pro-any amino acid-Tyr) (residues 962–965) motif and a YXXL (Tyr-any amino acid-any amino acid-Leu) (residues 1019–1022) motif (Figure 2). These motifs are present in the cytoplasmic domains of many transmembrane receptors and in many cases direct the phosphorylation of the tyrosine residue and mediate interactions with cytoplasmic adaptor proteins (Pawson and Scott, 1997).

No biological function or biochemical activity is known for mEGF6 or Y64G10A.7. SREC, by contrast, was identified in human endothelial cells as a scavenger receptor mediating the endocytosis of chemically modified lipoproteins and other polyanionic substrates (Adachi et al., 1997). In addition to sequence similarity with CED-1 in the extracellular domain, SREC also shares a similar overall structure with CED-1 (Figure 1B). Both contain an N-terminal extracellular domain, a single transmembrane domain, and a C-terminal intracellular domain. The similarity of these two proteins indicates that CED-1 may function as a receptor for extracellular ligands and possess ligand binding specificity similar to that of SREC.

Characterization of *ced-1* Alleles

We identified the molecular lesions associated with 15 *ced-1* alleles isolated by Hedgecock et al. (1983) and Ellis et al. (1991), confirming that we correctly identified the *ced-1* gene (Figure 1B and Table 1). The allele *e1754* contains a nonsense mutation at codon 32 and likely completely abolishes *ced-1* function, consistent with its strong cell corpse retention phenotype (Table 1).

The only known defect of *ced-1* mutants is the presence of persistent cell corpses. We examined the strength of this phenotype caused by different *ced-1* mutations (Table 1). The five distinct alleles (*e1799/e1800, n691, e1735, e1814*, and *e1798*) that presumably result in truncated CED-1 proteins as a consequence of nonsense, splicing, or frameshift mutations, cause an 84%–100% retention of cell corpses as compared to the null mutation *e1754*, indicating that deletions of the transmembrane and intracellular domains result in a total loss of *ced-1* function. Five of the six distinct missense mutations (*n2091, n2089, e1797/n2000/n2092, n1951*, and *e1801*) convert conserved cysteines to tyrosines in various EGF-like repeats, and the number of persistent corpses associated with these alleles is at least 70% that of null mutants. Cysteine residues in EGF-like repeats form disulfide bonds and are essential for the structural integrity of the protein (Campbell and Bork, 1993). These missense mutations may cause misfolding of CED-1 by creating unpaired cysteine residues and may even prevent CED-1 from being exported from the endoplasmic reticulum, thereby resulting in a severe loss of CED-1 function.

Our more thorough phenotypic analysis of two representative alleles, the null allele *e1754* and the strongest missense allele *n2089*, established that cell corpses persisted throughout the body, including in the posterior ventral cord and tail in larvae and in the germline in adults (Table 2 and data not shown). These results indicate that *ced-1* is required for the engulfment of all cell corpses.

We analyzed a large number of cell corpses in *ced-1* mutant animals using transmission electron microscopy. In the gonad of the adult hermaphrodite, in wild-type animals cell corpses disappear rapidly after formation and those found are seen within gonadal sheath cells as phagosomes (Figures 3A and 3D); by contrast, in *ced-1(e1754)* animals, 29 of 31 germ cell corpses remained unengulfed, although short extensions from the gonadal sheath cells were often seen in contact with the corpses (Figures 3B and 3E). The other two corpses were found within gonadal sheath cells (data not shown).

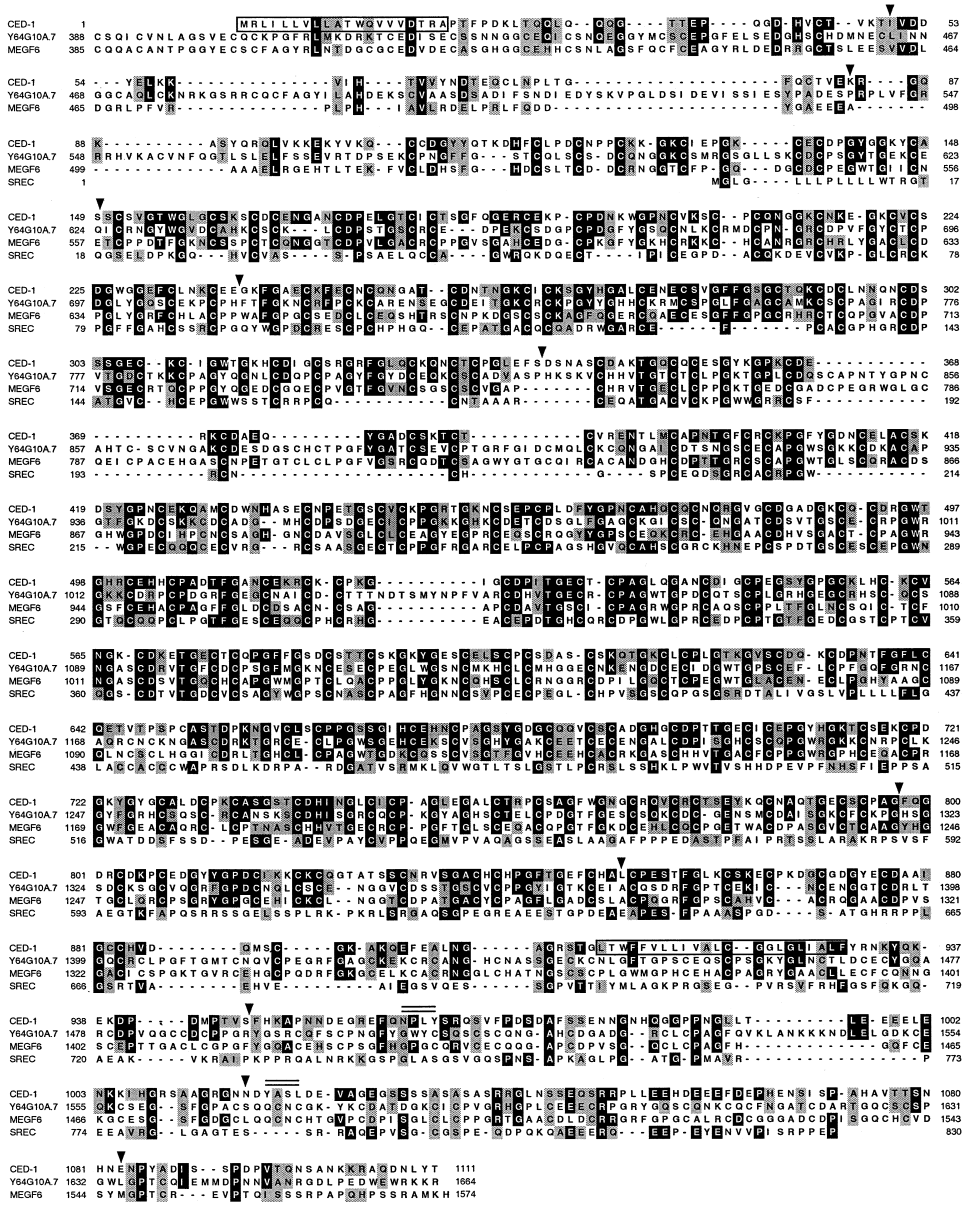

Figure 2. Sequence Alignment of CED-1 and Related Proteins

Numbers indicate amino acid positions. Residues identical or similar in CED-1 and other proteins are shaded in black or gray, respectively. Dashes indicate gaps. The predicted signal sequence and transmembrane domain are boxed. Arrowheads indicate the positions of introns. The NPXY and YXXL motifs are indicated by double lines on top.

We then examined cell corpses formed in the tail and corpses descended from the ventral cord precursor cells P9 through P12 at the L3 stage, at which point these corpses had persisted for at least 12 hr. Among the 17 corpses examined, 16 remained unengulfed. These unengulfed corpses were nevertheless in close contact with and often partially enveloped by their living neighbors, and in some cases short pseudopod-like structures extended from the neighboring cells and partially surrounded the corpses (Figures 3C and 3F). These results indicate that the major defect of *ced-1* mutants is in the engulfment, not the digestion, of cell corpses, consistent with previous observations (Hedgecock et al., 1983). Our results further indicate that engulfment was perturbed, but not abolished, in *ced-1* mutants since engulfing cells still partially extended membranes around cell corpses.

CED-1 Is Localized to Cell Surfaces and Expressed at High Levels in Cell Types that Can Function as Engulfing Cells

To study the subcellular localization and expression pattern of CED-1, we analyzed a CED-1::GFP (*g*reen *f*luorescence *p*rotein; Chalfie et al., 1994) fusion protein under the control of the *ced-1* promoter ($P_{ced\text{-}1}$*ced-1::gfp*, see Experimental Procedures). The expression of this construct in *ced-1* mutants fully rescued the engulfment defects (Table 5), indicating that the CED-1::GFP fusion

Table 1. *ced-1* Molecular Lesions and Mutant Phenotypes

Allele	Nucleotide and Amino Acid Changes[a]	Codon Position	No. Corpses in L1 Head
e1754	CAG (Q) to TAG (stop)	32	26.7 ± 4.4 (n = 9)
n1995	CCG (P) to CTG (L)	124	13.2 ± 3.3 (n = 10)
n2091	TGT (C) to TAT (Y)	136	15.9 ± 2.9 (n = 14)
e1799, *e1800*	AGgtaga to AGataga, splice donor	239	24.9 ± 2.7 (n = 10)
n691	C missing, frameshift	261	25.3 ± 4.1 (n = 12)
n2089	TGT (C) to TAT (Y)	330	27.5 ± 3.6 (n = 20)
e1735	CAA (Q) to TAA (stop)	375	27.4 ± 2.6 (n = 10)
e1797, *n2000*, *n2092*	TGC (C) to TAC (Y)	448	22.8 ± 2.9 (n = 10)
n1951	TGT (C) to TAT (Y)	501	18.2 ± 3.7 (n = 10)
e1814	CAG (Q) to TAG (stop)	686	22.3 ± 4.1 (n = 12)
e1801	TGT (C) to TAT (Y)	803	20.3 ± 3.8 (n = 12)
e1798	CAA (Q) to TAA (stop)	887	25.1 ± 6.4 (n = 9)
wild-type	NA	NA	0 (n = 20)

[a] Mutated nucleotides are underlined. Nucleotides in lowercase letters represent intron sequences. The encoded amino acids are represented by single letter abbreviations in parentheses.
Numbers of persistent cell corpses are presented as mean ± standard deviation. n, number of animals scored. NA, not applicable.

protein preserved the activity of CED-1. The GFP signal was localized to cell surfaces in all cells in which expression was detected (Figures 4A–4F), indicating that CED-1 is a transmembrane protein, as predicted by its amino acid sequence.

We observed broad expression of $P_{ced\text{-}1}$*ced-1::gfp* during development. *ced-1* was expressed at high levels in cells that can function as engulfing cells. Hypodermal cells, which form an outer monolayer of the animal's body, are responsible for engulfing most somatic cell corpses, and intestinal and pharyngeal muscle cells also act as engulfing cells (Robertson and Thomson, 1982; Sulston et al., 1983). The earliest GFP signal observed was in the four intestinal precursor cells in 50 to 100 cell stage embryos (Figure 4A). Embryonic cell deaths occur during mid-embryogenesis between the 250-cell and 550-cell stages (Sulston et al., 1983). In embryos at the 250-cell stage or older, CED-1::GFP was visible in hypodermal cells (Figure 4B), intestinal cells, and the entire pharyngeal primordium (Figure 4C). This expression pattern persisted until hatching. During larval development, intestinal cell expression diminished, but expression in hypodermal cells and in all pharyngeal cells remained strong (Figure 4D). GFP signal was also observed in body wall and vulval muscles, and in many neurons in the head and ventral nerve cord (data not shown).

In L4 larvae and adult hermaphrodites, the strongest CED-1::GFP signal was observed on the surfaces of the gonadal arms (Figures 4E and 4F). To distinguish whether this signal was from the germline syncytium or from the gonadal sheath cells, which form a thin layer that covers most of the germline (Hall et al., 1999) and which are solely responsible for engulfing germ cell corpses (Gumienny et al., 1999), we analyzed a $P_{ced\text{-}1}$*NLS-gfp* construct in which a GFP protein expressed from the *ced-1* promoter was predominantly localized to the nucleus (see Experimental Procedures). We detected GFP signal within the nuclei of all gonadal sheath cells but not within any germ cell nuclei (Figure 4G). This result suggests that *ced-1* is highly expressed in the gonadal sheath cells and localizes to the surfaces of these cells. In addition, $P_{ced\text{-}1}$*ced-1::gfp* was expressed in the cells of the spermatheca and uterus (data not shown).

We used the $P_{ced\text{-}1}$*NLS*-gfp reporter to determine whether CED-1 was also present in cell corpses. The temporal expression pattern and tissue distribution of this construct were identical to that of $P_{ced\text{-}1}$*ced-1::gfp*. In wild-type embryos at the bean-comma stage (~550-cells), zero of 14 visible corpses were GFP positive. In addition, on average only one of 26 persistent cell corpses was GFP positive in the heads of *ced-1* mutants at the L1 larval stage, indicating that CED-1 was absent

Table 2. Expression of *ced-1* cDNA in Engulfing but Not Dying Cells Rescued a *ced-1* Phenotype

Genotype	Transgene[a]	No. corpses		
		Head of L2 Larvae	Posterior Ventral Cord of L3 Larvae	Germline of Adults[b]
ced-1 (+)	–	0 (n = 20)	0 (n = 20)	3.9 ± 1.6 (n = 15)
ced-1 (*n2089*)	–	27.1 ± 3.1 (n = 15)	5.0 ± 0.9 (n = 20)	60.2 ± 15.6 (n = 15)
ced-1 (*n2089*)	$P_{col\text{-}10}$*ced-1::gfp*	2.9 ± 1.4 (n = 12)	0 (n = 10)	66.0 ± 11.4 (n = 11)
ced-1 (*n2089*)	$P_{lim\text{-}7}$*ced-1::gfp*	ND	4.9 ± 0.9 (n = 10)	4.4 ± 2.8 (n = 10)
ced-1 (*n2089*)	$P_{egl\text{-}1}$*ced-1::gfp*	ND	4.7 ± 0.6 (n = 11)	60.0 ± 14.0 (n = 12)

[a] For each transgene construct, two independent lines were assayed and found to have similar phenotypes, and the results of one line are reported. –, no transgene.
[b] Scored in one gonadal arm of each adult hermaphrodite two days after L4 molt.
Data are presented as mean ± standard deviation. n, number of animals scored. ND, not determined.

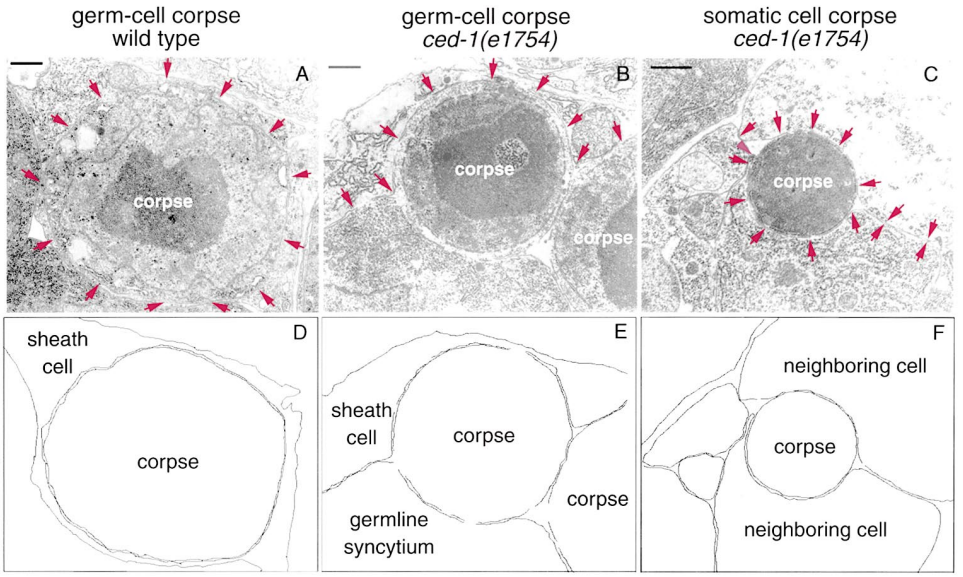

Figure 3. Cell Corpses Remain Unengulfed in *ced-1* Mutants

(A–C) Transmission electron micrographs of cell corpses. The membranes of neighboring cells surrounding the corpses are indicated by arrows. (A) A germ cell corpse engulfed by a gonadal sheath cell in a wild-type adult hermaphrodite. (B) An unengulfed germ cell corpse in the gonad of a *ced-1(e1754)* adult hermaphrodite, surrounded by a gonadal sheath cell (arrows), another cell corpse, and the germline syncytium. (C) An unengulfed cell corpse in the tail of an L3-stage *ced-1(e1754)* larva. The cell at the bottom in contact with the corpse extends one pseudopod-like structure (arrowhead) along the corpse. The cytoplasmic structures of the cell on the top were lost during fixation. (D–F) Traces of the membranes of the cell corpses and their neighboring engulfing cells shown in (A)–(C), respectively.

from most cell corpses, at least at the stages of programmed cell death at which cell corpses are distinguishable using Nomarski optics.

ced-1 Functions in Engulfing but Not Dying Cells

To determine whether *ced-1* acts in dying cells, engulfing cells, or both for engulfment, we examined where *ced-1* must be expressed to rescue the engulfment defect of *ced-1* mutants. We tested three cell type-specific promoters: $P_{col\text{-}10}$, $P_{lim\text{-}7}$, and $P_{egl\text{-}1}$. $P_{col\text{-}10}$, the promoter for the collagen gene *col-10* (V. Ambros, personal communication), is specific for hypodermal cells. $P_{lim\text{-}7}$, the promoter for the HOX gene *lim-7*, is predominantly expressed in gonadal sheath cells (Hall et al., 1999). $P_{egl\text{-}1}$, which includes the promoter and downstream regulatory sequences of the cell death activator *egl-1* (Conradt and Horvitz, 1999), is expressed predominantly in somatic dying cells (B. Conradt and H. R. Horvitz, personal communication). Using these promoters, we expressed a CED-1::GFP fusion protein with complete *ced-1* rescuing activity. The cell type specificity of these promoters was confirmed by monitoring the GFP signal (data not shown). Hypodermal cell-specific expression of CED-1::GFP ($P_{col\text{-}10}$*ced-1::gfp*) resulted in complete engulfment of somatic cell corpses in the posterior ventral cord and almost complete engulfment in the head, but no engulfment of germ cell corpses (Table 2). Among the seven cells that die in the posterior ventral cord and the 93 cells that die in the head, only one cell is derived from the hypodermal lineage (Sulston and Horvitz, 1977; Sulston et al., 1983). Therefore, the rescuing activity was not expressed within these dying cells. CED-1::GFP expression in the gonadal sheath cells ($P_{lim\text{-}7}$*ced-1::gfp*) fully rescued germ cell corpse engulfment but not somatic cell corpse engulfment (Table 2). We observed no significant rescue of the engulfment defect of either somatic or germ cell corpses after $P_{egl\text{-}1}$*ced-1::gfp* expression (Table 2), despite the fact that CED-1::GFP was observed in cell corpses (data not shown). Together, these results indicate that expression of *ced-1* in engulfing cells but not in dying cells is sufficient for engulfment. We conclude that *ced-1* functions in engulfing cells.

CED-1 Clusters around Cell Corpses

We used the CED-1::GFP fusion protein to monitor the localization of CED-1 in living animals in which cell corpses are distinguishable using Nomarski optics. In wild-type embryos expressing $P_{ced\text{-}1}$*ced-1::gfp*, a very bright GFP signal was detected along the surfaces of cell corpses (Figures 5A and 5B). Quantitative analyses indicated that the intensity of the GFP signal along the surfaces of cell corpses was on average 2.3 $\pm$ 0.4-fold as strong as that on the surfaces of their neighboring, living cells (Figures 5C–5F). By analyzing serial optical sections of embryos, we found that most of these bright corpses were inside living cells (Figures 5G–5L), consistent with the report that engulfment occurs rapidly after cell death (Sulston et al., 1983). Our analysis of $P_{ced\text{-}1}$*NLS-gfp* expression suggested that CED-1 is absent from most cell corpses (Table 3 and above). Therefore, the bright GFP signal surrounding cell corpses presumably originates from the surfaces of neighboring cells. In support of this hypothesis, CED-1::GFP expressed from the heatshock promoters (P_{hsp}*ced-1::gfp*) after cell corpses had formed and at a time at which macromolecular synthesis no longer occurs in the corpses (Wu and Horvitz, 1998b) labeled persistent cell corpses in *ced-6*

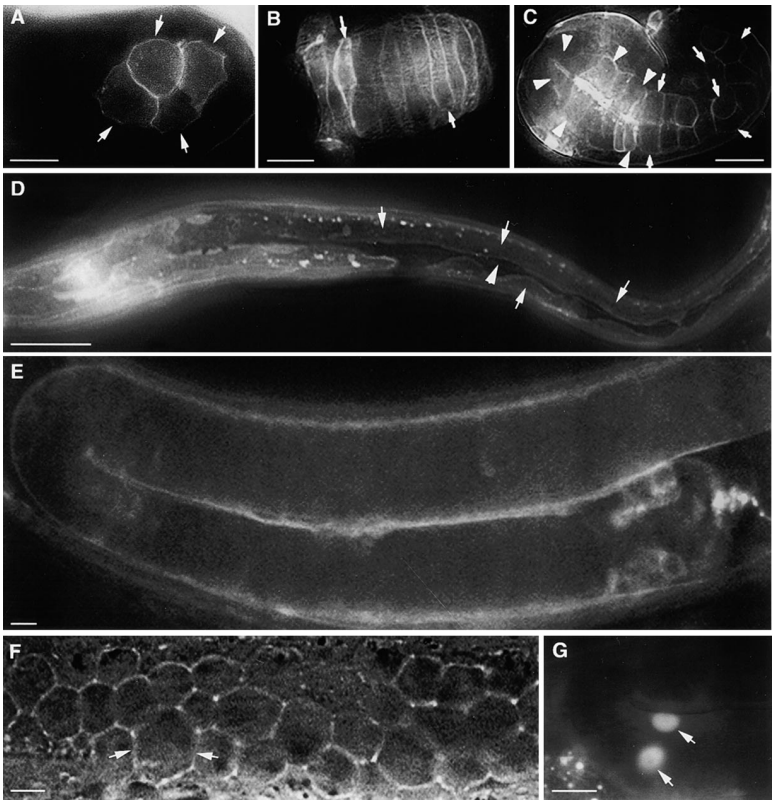

Figure 4. CED-1 Is Highly Expressed in Engulfing Cells and Localized to Cell Surfaces

(A–F) $P_{ced\text{-}1}$*ced-1::gfp* expression in wild-type animals was visualized by epifluorescence. Anterior is to the left. Scale bar: 10 μm. (A) A 50–100 cell stage embryo. Arrows indicate four intestinal cells that express CED-1::GFP. (B) GFP signal on the surface of dorsal hypodermal cells (two are indicated by arrows) in an ~500 cell stage embryo. (C) GFP signal in all 20 intestinal cells (six are indicated by arrows; only two of the four intl cells are visible) and the entire pharynx primordium (arrowheads) in a 1.5-fold stage embryo (~550 cells). (D) L1 larva. Syncytium hypodermal cells strongly express CED-1::GFP (arrows). Arrowhead indicates the position of a lateral seam cell that weakly expresses CED-1::GFP. (E–F) Gonad arm in an adult hermaphrodite. Dorsal is up. (E) Mid-focal plane view showing GFP signal in the gonadal sheath cells. (F) Surface view of the distal region of a gonadal arm; two arrowheads mark part of a sheath cell that chelates between the germ cells. (G) $P_{ced\text{-}1}$*NLS-gfp* expression in the nuclei of gonadal sheath cells (arrows) visualized by epifluorescence. Dorsal is up. Scale bar: 10 μm.

mutant animals, which are defective for cell corpse engulfment (Ellis et al., 1991) (Table 3 and Figures 6A–6E). In addition, CED-1::GFP expressed in hypodermal cells ($P_{col\text{-}10}$*ced-1::gfp*), a major engulfing cell type, labeled the surface of persistent cell corpses (Table 3). These observations suggest that CED-1::GFP on the membranes of neighboring cells clusters around cell corpses. Our electron microscopic studies indicate that in engulfment mutants, cells that normally engulf dying cells are still in close contact with dying cells. Pseudopod-like structures from such neighboring cells were often seen to partially surround cell corpses (Figure 3). This observation predicts that partial CED-1::GFP circles might be present around persistent cell corpses, as is indeed the case (Figures 6A–6E). However, we also observed full GFP-positive circles around cell corpses in engulfment-deficient mutants (Figures 6A and 6B). Perhaps in these cases the clustering of CED-1 expressed on the surface of two or more neighboring cells resulted in a combined full GFP-positive circle. We noted that the GFP signal around an engulfed corpse was always a full circle (Figure 5), consistent with our electron microscopic observation of a phagosome-like structure in which an engulfed corpse was completely surrounded by membrane originated from the plasma membrane of the engulfing cell (Figures 3A and 3D).

CED-1::GFP Fails to Cluster around Cell Corpses in *ced-7* Mutant Animals

As noted above, mutants defective in the engulfment gene *ced-6* appeared normal in the clustering of CED-1 around persistent cell corpses (Table 3 and Figures 6A–6E), indicating that clustering does not require complete engulfment and that *ced-6* function is not needed for CED-1 clustering. We similarly asked if other engulfment genes are needed for CED-1 clustering. We introduced P_{hsp}*ced-1::gfp*, a rescuing construct, into engulfment mutants defective in *ced-2*, *ced-5*, *ced-7*, or *ced-10* and assayed for CED-1 clustering after induction of transgene expression (Table 4). In all of these mutants, CED-1::GFP expression was dependent on heat shock and displayed an intensity and pattern identical to those in wild-type animals. Induced CED-1::GFP expression did not rescue the engulfment defect of any of these mutants (Table 4). In *ced-2*, *ced-5*, and *ced-10* mutants, GFP-positive cell corpses were detectable in the heads of larvae starting from the L1 stage, indicating that the clustering of CED-1::GFP around cell corpses was not severely affected. By contrast, although in *ced-7* mutant animals CED-1::GFP was localized to cell surfaces (Figure 6F), indicating that mutation of *ced-7* did not affect the plasma-membrane localization of CED-1, strikingly, we failed to detect GFP-positive cell corpses (Table 4) (Figures 6F and 6G). Similarly, using the reporter construct $P_{ced\text{-}1}$*ced-1::gfp*, the expression pattern and subcellular localization of which were also wild type in *ced-7* mutants, we again observed that the clustering of CED-1::GFP was greatly diminished (Table 4). These results indicate that the function of *ced-7* is necessary for CED-1 to cluster around cell corpses.

The Intracellular Domain of CED-1 Is Essential For Cell Corpse Engulfment but Not Recognition or for CED-1 Clustering around Cell Corpses

We expressed a truncated form of CED-1 lacking the intracellular domain (residues 931–1111) as a GFP fusion

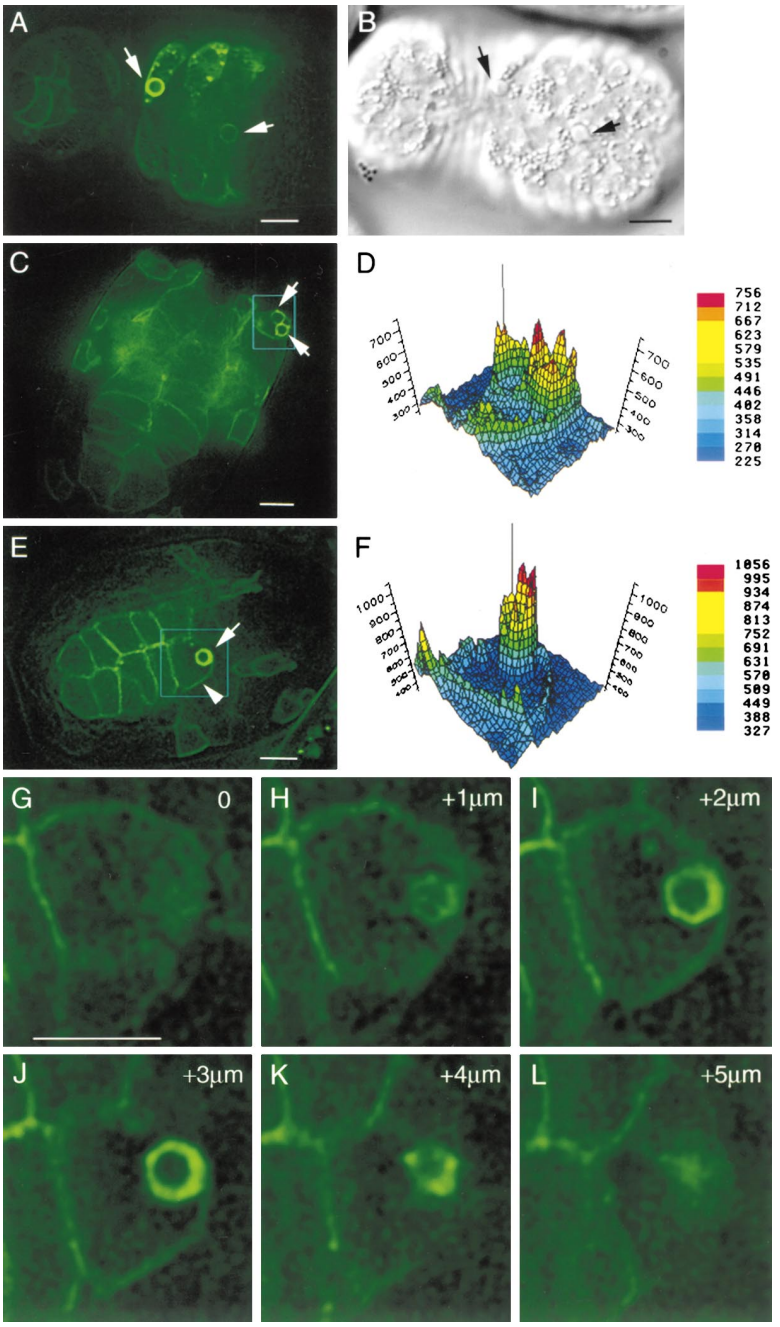

Figure 5. CED-1::GFP Clusters around Cell Corpses

P_{ced-1}ced-1::gfp was expressed in wild-type embryos. GFP was visualized by epifluorescence. Anterior is to the right. Scale bar: 5 μm.

(A and B) A bean stage (~550 cells) embryo. Arrows mark two GFP-positive cell corpses inside ventral hypodermal cells. (A) Epifluorescence. (B) Nomarski image.

(C and E) Epifluorescence. (C) Two corpses (arrows) and the cell that has engulfed them in a ~500 to ~550 cell stage embryo are boxed. (E) An anterior intestinal cell (arrowhead) and a GFP-positive cell corpse inside it (arrow) in a ~350 cell stage embryo are boxed. (D and F) Quantitation of GFP signal intensity within the boxed regions in (C) and (E), respectively. GFP intensity is marked on the Z-axis and represented by various colors indicated on the right. The boxed areas are presented as being rotated 45° counterclockwise.

(G–L) Epifluorescence. Serial Z-sections (1 μm intervals) of the boxed region in (E) presented in a 3.5-fold magnification.

under P_{ced-1} control (*P_{ced-1}ced-1ΔC::gfp*). This construct did not rescue the engulfment defect of *ced-1(e1754)* or *ced-1(n2089)* animals (Table 5 and data not shown). However, its temporal and spatial expression pattern was identical to that of *P_{ced-1}ced-1::gfp* (Figures 7A and 7B and data not shown). CED-1ΔC::GFP was membrane localized (Figure 7A) and clustered around transient cell corpses (Figure 7B), just as did CED-1::GFP. CED-1ΔC::GFP also clustered around persistent cell corpses (Table 5). These results indicate that the extracellular and transmembrane domains of CED-1 are sufficient for clustering around cell corpses and that the intracellular domain is essential for corpse engulfment although not for clustering. A second truncated form of CED-1 lacking both the transmembrane and intracellular domains (residues 909–1111) as a GFP fusion (*P_{ced-1}ced-1Ex::gfp*) similarly did not rescue the *ced-1(e1754)* mutant phenotype (Table 5). Furthermore, the GFP signal was not localized to cell surfaces, but instead appeared diffuse and very weak (Figure 7C), and GFP-positive cell corpses were not observed (Table 5), indicating that the predicted transmembrane domain (residues 909–930) is required for the membrane localization of CED-1 and for its clustering around cell corpses. The expression of both CED-1ΔC::GFP and CED-1Ex::GFP in wild-type animals resulted in weak yet significant engulfment defects not observed in animals expressing the full-length CED-1::GFP (Table 5). We suggest that these truncated forms

Table 3. CED-1::GFP Localized on the Surface of Neighboring Cells Clusters around Persistent Cell Corpses

	No. Corpses in L3 Head	
Transgene[a]	GFP-Positive	Total
P_{ced-1}*ced-1::gfp*	11.8 ± 3.1 (n = 12)	18.2 ± 2.3 (n = 12)
P_{col-10}*ced-1::gfp*	6.2 ± 3.0 (n = 10)	17.5 ± 1.4 (n = 10)
P_{ced-1}*NLS-gfp*	0.9 ± 0.9 (n = 12)	17.8 ± 2.0 (n = 12)
P_{hsp}*ced-1::gfp*[b]	10.7 ± 3.3 (n = 11)	17.9 ± 4.4 (n = 11)
P_{hsp}*gfp*[2]	0 (n = 12)	17.5 ± 1.6 (n = 12)
None	NA	17.4 ± 2.4 (n = 15)

[a] Two independent lines of each transgene were scored in a *ced-6(n2095)* genetic background and found to have similar phenotypes, and the results of one line are reported.
[b] Heat shock was performed at 33°C for 1.5 hr using a mixed-staged population. After 9 hr of recovery at 20°C, mid-L3 stage transgenic animals were scored.
Data are presented as mean ± standard deviation. n, number of animals scored. NA, not applicable.

have dominant-negative effects and that the function of the endogenous wild-type CED-1 was perturbed by the truncated forms, possibly through competition for ligands and/or interference with signal transduction.

The Predicted PTB Binding and SH2 Binding Motifs of CED-1 Are Essential For CED-1 Function

We examined the functions of two conserved motifs in the intracellular domain of CED-1: the NPXY motif (residues 962–965), a potential PTB domain binding site, and the YXXL motif (residues 1019–1022), a potential site for tyrosine phosphorylation and binding to the SH2 domain (Pawson and Scott, 1997). We mutated conserved residues of each motif (N962, Y965, and Y1019) to alanine and introduced single and double mutations into the P_{ced-1}*ced-1::gfp* reporter. The N962A, Y965A, and Y1019A mutations resulted in 85%, 71%, and 54% loss of CED-1 activity, respectively (Table 5), indicating each of these three residues is necessary for the full engulfment activity of CED-1 and that the NPXY motif plays a more major role. The N962A Y1019A and Y965A Y1019A double mutations caused 100% inactivation of CED-1, suggesting that the NPXY and YXXL motifs are partially redundant in function. None of the mutations affected the clustering of CED-1::GFP around cell corpses (Table 5), consistent with our observation that the intracellular domain of CED-1 is not necessary for the recognition of cell corpses and suggesting that the intracellular domain controls downstream signal transduction to activate the cell corpse internalization process.

Discussion

CED-1 Is a Receptor that Recognizes Cell Corpses

The predicted CED-1 protein bears structural resemblance to many transmembrane receptors, including growth factor receptors, integrins, and lipoprotein receptors. The large CED-1 extracellular domain contains 16 copies of an atypical type of EGF-like repeat. Many cell surface receptors contain multiple extracellular EGF-like repeats, which are important for ligand recep-

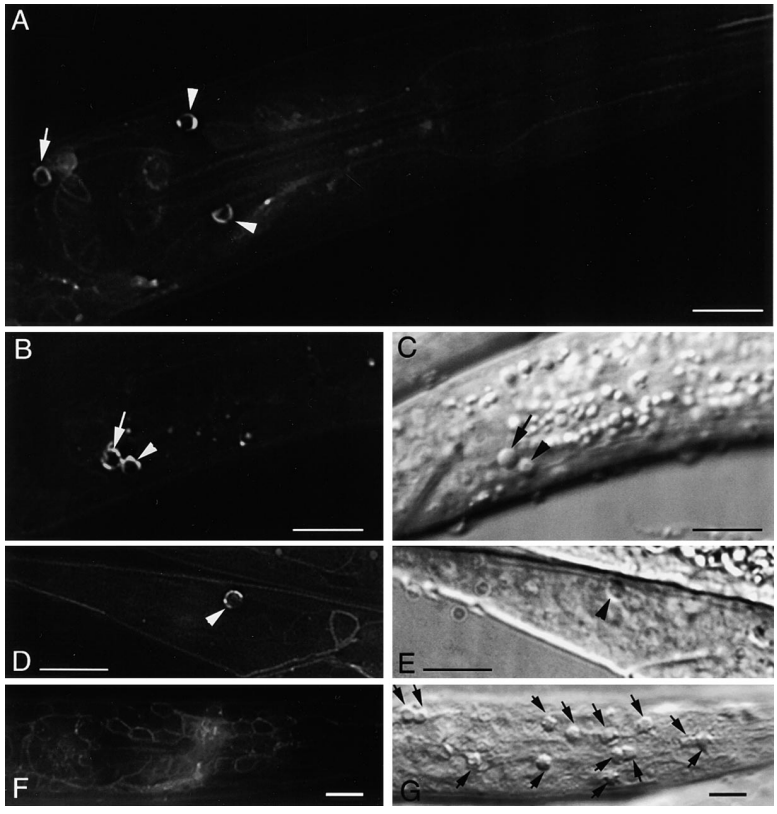

Figure 6. CED-1::GFP Clusters around Cell Corpses in *ced-6* but Not *ced-7* Mutants

ced-6(n2095) (A–E) and *ced-7(n1996)* (F and G) animals were induced to express P_{hsp}*ced-1::gfp*. GFP was visualized by epifluorescence. Anterior is to the right, dorsal is up. Scale bar: 5 μm. (A, B, D, and F) Epifluorescence. (C, E, and G) Nomarski images. (A–E) Arrows indicate full GFP-positive circles. Arrowheads indicate partial GFP-positive circles. (A) Head of an L3 larva. The GFP signal around persistent cell corpses was produced at least 15 hr after cell death. (B and C) Posterior ventral cord of an L2 larva. (D and E) Tail of an L1 larva. (F and G) Head of a *ced-7(n1996)* L1 larva. Arrows indicate the positions of cell corpses. No CED-1::GFP clustering was detected around any corpses.

Table 4. The Clustering of CED-1::GFP around Cell Corpses Is Abolished in *ced-7* Mutants

Genotype	Transgene[a]	No. Corpses in L1 Head	
		GFP-Positive	Total
ced-2(e1752)	P_{hsp}*ced-1::gfp*[b]	7.5 ± 6.8 (n = 12)	23.0 ± 3.6 (n = 12)
ced-5(n1812)	P_{hsp}*ced-1::gfp*[b]	6.9 ± 4.5 (n = 8)	29.3 ± 5.8 (n = 8)
ced-6(n2095)	P_{hsp}*ced-1::gfp*[b]	6.8 ± 2.5 (n = 11)	22.3 ± 2.3 (n = 11)
ced-7(n1996)	P_{hsp}*ced-1::gfp*[b]	0.2 ± 0.6 (n = 10)	17.8 ± 4.5 (n = 10)
ced-10(n3246)	P_{hsp}*ced-1::gfp*[b]	4.4 ± 1.6 (n = 8)	25.1 ± 2.5 (n = 8)
ced-6(n2095)	$P_{ced\text{-}1}$*ced-1::gfp*	7.9 ± 3.0 (n = 11)	20.1 ± 4.0 (n = 11)
ced-7(n1996)	$P_{ced\text{-}1}$*ced-1::gfp*	1.1 ± 1.3 (n = 11)	22.0 ± 4.8 (n = 11)

[a] For each transgene construct, two independent lines were scored and found to have similar phenotypes, and the results of one line are reported.
[b] Heat shock was performed at 33°C for 1.5 hr using a mixed-staged population. After 9 hr of recovery at 20°C, mid-L1 stage transgenic animals were scored.
Data are presented as mean ± standard deviation. n, number of animals scored.

tor interaction (Campbell and Bork, 1993; Kimble et al., 1998). The extracellular domain of CED-1 may likewise function as a ligand recognition domain. The presence of the NPXY and YXXL motifs in the predicted intracellular domain of CED-1 suggests that this domain, like that of many transmembrane receptors, mediates signal transduction by interacting with cytoplasmic adaptor proteins (Pawson and Scott, 1997). These structural features suggest that CED-1 acts as a transmembrane receptor. We propose that CED-1 is a receptor on the surface of engulfing cells and acts to recognize cell corpses. Our results show that CED-1 is localized to cell surfaces and that its predicted transmembrane domain is required for this localization. *ced-1* is expressed and functions in engulfing but not dying cells. Importantly, a CED-1::GFP fusion protein on the surfaces of neighboring cells clusters around cell corpses, and this clustering requires the extracellular and transmembrane domains but not the intracellular domain of CED-1, indicating that the clustering is a direct response to an extracellular signal that distinguishes cell corpses from living cells. Both the NPXY and YXXL motifs are necessary for the function of the intracellular domain of CED-1, strongly suggesting the presence of an intracellular signal transduction pathway.

CED-1 Is Similar to Mammalian Scavenger Receptors

Mammalian scavenger receptors were first identified by their abilities to mediate the endocytosis of chemically modified lipoproteins and other polyanionic substances (reviewed by Krieger and Herz, 1994). At least six structurally distinct classes have been identified from macrophages and other cell types, and multiple physiological roles, including lipoprotein metabolism, cell adhesion, host defense, and recognition of apoptotic cells, have been indicated (Krieger and Herz, 1994; Platt et al., 1998). In in vitro assays, SR-A (a Class A receptor), CD36 and SR-BI/CLA-1 (Class B), CD68 (Class D), and LOX-1 (Class E) can mediate the recognition and phagocytosis of apoptotic cells (Ren et al., 1995; Sambrano and Steinberg, 1995; Platt et al., 1996; Murao et al., 1997;

Table 5. The Intracellular Domain of CED-1 is Essential for Signal Transduction Events Downstream of Cell Corpse Recognition

Genotype	Transgene[a]	No. Corpses in the Head	
		GFP-Positive	Total
ced-1(e1754)[b]	*ced-1::gfp*	0.1 ± 0.3 (n = 12)	0.4 ± 0.8 (n = 12)
ced-1(e1754)[b]	*ced-1ΔC::gfp*	8.9 ± 2.2 (n = 12)	16.8 ± 2.6 (n = 12)
ced-1(e1754)[b]	*ced-1Ex:gfp*	0.2 ± 0.4 (n = 10)	17.5 ± 3.2 (n = 10)
ced-1(e1754)[b]	None	NA	17.9 ± 2.4 (n = 12)
wild-type[c]	*ced-1::gfp*	0.2 ± 0.4 (n = 15)	0.2 ± 0.4 (n = 15)
wild-type[c]	*ced-1ΔC::gfp*	1.9 ± 1.4 (n = 15)	2.3 ± 1.6 (n = 15)
wild-type[c]	*ced-1Ex::gfp*	0.3 ± 0.6 (n = 15)	1.0 ± 1.4 (n = 15)
wild-type[c]	None	NA	0.1 ± 0.3 (n = 15)
ced-1(e1735)[c]	*ced-1::gfp*	0.1 ± 0.3 (n = 15)	0.1 ± 0.3 (n = 15)
ced-1(e1735)[c]	*ced-1*(N962A)*::gfp*	10.1 ± 2.3 (n = 15)	23.3 ± 2.2 (n = 15)
ced-1(e1735)[c]	*ced-1*(Y965A)*::gfp*	8.4 ± 1.6 (n = 14)	19.6 ± 3.0 (n = 14)
ced-1(e1735)[c]	*ced-1*(Y1019A)*::gfp*	9.7 ± 2.4 (n = 15)	14.8 ± 4.2 (n = 15)
ced-1(e1735)[c]	*ced-1*(N962A Y1019A)*::gfp*	7.9 ± 2.3 (n = 15)	27.7 ± 3.6 (n = 15)
ced-1(e1735)[c]	*ced-1*(Y965A Y1019A)*::gfp*	7.6 ± 2.2 (n = 12)	27.5 ± 2.4 (n = 12)
ced-1(e1735)[c]	None	NA	27.5 ± 3.6 (n = 15)

[a] All transgenes were expressed from the *ced-1* promoter ($P_{ced\text{-}1}$) (see Experimental Procedures). For each transgene construct, two independent lines were scored and found to have similar phenotypes, and the results of one line are reported.
[b] Animals were scored at L3 larval stage.
[c] Animals were scored at L1 larval stage because the greatest number of cell corpses is present at the L1 stage, allowing better scoring of partial engulfment defects.
Data are presented as mean ± standard deviation. n, number of animals scored. NA, not applicable.

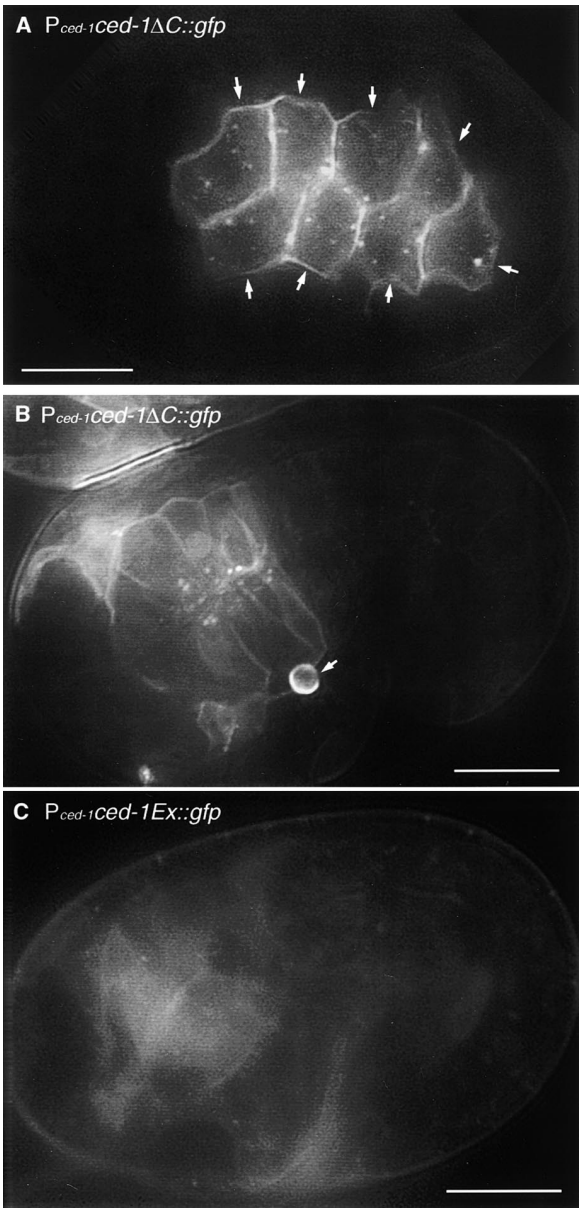

Figure 7. The Extracellular and Transmembrane Domains of CED-1 Are Sufficient for CED-1::GFP to Cluster around Cell Corpses

Reporter constructs expressed in wild-type embryos are indicated on the top of each panel. GFP was visualized by epifluorescence. Anterior is to the left. Scale bar: 10 μm.

(A) Intestinal cells (arrows) in a 150 to 200 cell stage embryo.

(B) A GFP-positive cell corpse (arrow) in a bean-stage (~550 cells) embryo.

(C) A 1.5 fold-stage (~550 cells) embryo.

Oka et al., 1998). In addition, CD36, SR-BI, and CD68 are known to recognize anionic phospholipids including phosphatidylserine (Tait and Smith, 1999 and references therein). The sequence similarity between CED-1 and human SREC suggests that these two proteins may possess similar ligand binding specificities. Furthermore, phosphatidylserine is a surface marker of mammalian apoptotic cells (Fadok et al., 1998). The strong conservation of mechanisms responsible for programmed cell death between *C. elegans* and mammals (reviewed by Metzstein et al., 1998) suggests that the signals presented on the surfaces of cell corpses could well be the same. Thus, phosphatidylserine may be a CED-1 ligand. The observed sequence similarity among CED-1, SREC, mEGF6, and Y64G10A.7 also suggests that human SREC, the single member of the Class F of scavenger receptors, and other proteins structurally related to CED-1 may be involved in the phagocytosis of apoptotic cells.

CED-7 Is Important for the Recognition of Cell Corpses by Engulfing Cells

In *ced-7* mutants, CED-1 failed to cluster around cell corpses, despite the fact that the expression pattern and subcellular localization of CED-1 were normal. This failure presumably reflects a primary defect in the ability of CED-1 to recognize cell corpses or to cluster around them. Genetic mosaic analysis indicated that *ced-7* is required in both dying and engulfing cells (Wu and Horvitz, 1998a). *ced-7* is the only engulfment gene known to play a role in dying cells. CED-7 is similar to ABC transporters, which effect ATP-dependent translocation of specific substrates across cellular membranes, is broadly expressed during embryogenesis, and is localized to plasma membranes (Wu and Horvitz, 1998a). We propose two possible mechanisms of CED-7 action: CED-7 may facilitate the physical contact between dying and engulfing cells by exporting unknown adhesive molecules from both; alternatively, CED-7 may perform different functions in dying and engulfing cells, e.g., acting in dying cells to present a cell corpse signal onto the cell surface, and in engulfing cells to assist CED-1 in recognizing its ligand and/or clustering around cell corpses. ABC1, the known mammalian protein most similar to CED-7, is involved in macrophage phagocytosis of apoptotic cells (Hamon et al., 2000). ABC1 promotes a transbilayer redistribution of phosphatidylserine and mediates the export of cholesterol and phospholipids from cells (Hamon et al., 2000). The Rim/ABCR protein, another mammalian protein similar to CED-7, acts as an outwardly directed membrane flippase for selected phospholipids (Weng et al., 1999). As discussed above, phosphatidylserine, an apoptotic cell surface marker, may be a CED-1 ligand. We propose that one role of CED-7 is to help present a cell corpse signal, perhaps phosphatidylserine, on the surface of dying cells by a flippase or transporter activity.

The CED-1 Signal Transduction Pathway

The clustering of mammalian phagocytic receptors that recognize opsonized-foreign particles, for example, the Fcγ receptor (FcγR), triggers downstream phosphorylation events that lead to cytoskeletal reorganization and the extension of pseudopodia around the surfaces of the particles (reviewed by Kwiatkowska and Sobota, 1999). It has not been established whether or not similar clustering occurs when phagocytic receptors recognize apoptotic cells. Our study of CED-1 shows that cell corpse receptors indeed cluster around their target apoptotic cells and strongly suggests that the clustering of CED-1 is important for recruiting downstream effectors and activating cell corpse engulfment.

What are these downstream effectors? The YXXL motif in the intracellular domain of CED-1 resembles the phosphorylation sites for the v-Src, Lck, and EGF receptor tyrosine kinases, which when phosphorylated bind to SH2 domain-containing adaptor proteins (Zhou and Cantley, 1995). Similarly, the intracellular domain of the receptor FcγR contains two nearby YXXL motifs shown from deletion and mutational analyses to be essential for FcγR function; phosphorylation of the two tyrosine residues plays an important role in the signaling that leads to a reorganization of the actin cytoskeleton (reviewed by Kwiatkowska and Sobota, 1999).

The intracellular domain of CED-1 also contains an NPXY motif, which is known to mediate binding to PTB domain-containing proteins, such as Shc, IRS-1, and Numb (Pawson and Scott, 1997). Recently, the NPXY motif was also found to act in novel signaling pathways critical for central nervous system development in mice (Trommsdorff et al., 1999). Specifically, the very low-density lipoprotein receptor (VLDLR) and the apolipoprotein E receptor 2 (ApoER2), two members of the LDL receptor family, use NPXY motifs in their intracellular domains to interact with the PTB domain-containing protein mDab1 (mouse Disabled-1) and activate intracellular signal transduction processes.

Our observation that the NPXY and YXXL motifs in the intracellular domain of CED-1 are essential for CED-1 function strongly implicates the involvement of downstream signal transduction molecules. We predict that Y1019 in the YXXL motif of CED-1 is phosphorylated in response to the recognition of cell corpses by CED-1 and that this phosphorylation recruits SH2 domain-containing proteins to CED-1 and activates a signal transduction cascade. Similarly, Y965 in the NPXY motif of CED-1 may be phosphorylated and recruit PTB domain-containing proteins; however, tyrosine phosphorylation is not a requirement for NPXY binding to some PTB domain-containing proteins (Pawson and Scott, 1997). The adaptor proteins that interact with the NPXY and YXXL motifs might regulate the same downstream signaling pathway cooperatively or might regulate different pathways. In either case, how these two motifs differentially contribute to the overall engulfment process should be of considerable interest.

ced-6 encodes a PTB domain-containing protein (Liu and Hengartner, 1998) and is in the same functional group as *ced-1* in the engulfment process (Ellis et al., 1991). Is CED-6 an adaptor that binds the NPXY motif of CED-1? We observed that a loss of *ced-6* function did not affect the ability of CED-1::GFP to recognize and cluster around cell corpses, consistent with the hypothesis that *ced-6* acts downstream of cell corpse recognition. However, in various in vitro assays, we have been unable to detect any physical interaction between CED-6 and the intracellular domain of CED-1 (Z. Z. and H. R. H., unpublished results). We suspect that the interaction between CED-1 and CED-6 is either indirect or requires an activated form of CED-1 induced by ligand engagement and clustering.

Reorganization of the actin cytoskeleton is an essential event in the extension of pseudopodia and thus could be one of the downstream events in the process of cell corpse engulfment regulated by CED-1. Cytoskeletal rearrangements that underlie cell membrane extensions in many if not all cases involve Rho/Rac-family GTPase signaling pathways (Van Aelst and D'Souza-Schorey, 1997). The molecular characterization of the *C. elegans* engulfment proteins CED-2 CrkII, CED-5 DOCK180, and CED-10 Rac GTPase revealed the involvement of a Rho/Rac-family GTPase complex in the signaling pathway for engulfment and most likely in cytoskeletal reorganization (Wu and Horvitz, 1998b; Reddien and Horvitz, 2000). However, CED-1 probably does not act, at least exclusively, to control the CED-2, CED-5, CED-10 pathway, as the effects of eliminating *ced-1* function are substantially enhanced by mutations in *ced-2, ced-5*, or *ced-10*, suggesting that CED-1 acts in a pathway that is parallel to and partially redundant with the CED-2, CED-5, CED-10 pathway (Ellis et al., 1991). Perhaps the CED-1 signaling pathway involves a different Rho-like GTPase, while the CED-2, CED-5, CED-10 pathway is triggered by a receptor that acts in parallel to CED-1.

Experimental Procedures

Mutations, Strains, and Transgenic Animals

C. elegans strains were cultured at 20°C as described by Brenner (1974). The N2 Bristol strain was used as the reference wild-type strain. The mutations used were as follows (Riddle et al., 1997): LG*I*, *unc-59(e261)*, *unc-75(e950)*, *ced-1(e1735, e1754, e1797, e1798, e1799, e1800, e1801, e1814)* (Hedgecock et al., 1983), *ced-1(n691, n1506, n1951, n1995, n2000, n2089, n2091, n2092)* (Ellis et al., 1991); LG*III*, *ced-6(n2095)*, *ced-7(n1996)*; LG*IV*, *ced-2(e1752)*, *ced-5 (n1812)*, *ced-10(n3246)*; LG*V*, *unc-76(e911)*. Germline transformation was performed as described by Mello et al. (1991). All strains used for introducing transgenes contained the *unc-76(e911)* mutation. Cosmids, fosmids, and *ced-1* expression constructs (at 20–80 ng/μl) were coinjected with the *unc-76* rescuing plasmid p76–16B (Bloom and Horvitz, 1997), and lines of non-Unc-76 transgenic animals were established.

Cloning of *ced-1*

See Supplementary Material at *Cell* website (http://www.cell.com/cgi/content/full/104/1/43/DC1).

Plasmid Construction

GFP vectors pPD95.67 and pPD95.75 and the P_{hsp}*gfp* constructs pPD99.44 and pPD99.52 were gifts from Dr. Andy Fire. We created a *ced-1* minigene by ligating an 8.7 kb *N*coI-ApaI fragment of *ced-1* genomic DNA containing 5 kb of the presumptive upstream regulatory region ($P_{ced\text{-}1}$) and the first three exons and introns to a 3.0 kb fragment of Form 1 *ced-1* cDNA starting from the fourth exon and ending at the poly(A) tail. This minigene fully rescued the engulfment defect of *ced-1(e1735)* mutant. An 11.2 kb HpaI-Sa*l*I fragment of this minigene was cloned into the GFP vector pPD95.67 to generate $P_{ced\text{-}1}$*ced-1::gfp,* which lacked residues 1052–1111 of CED-1 but fully rescued the engulfment defects of the *ced-1* mutants (Table 5). To generate $P_{ced\text{-}1}$*ced-1*Δ*C::gfp*, we inserted a SmaI site into the *ced-1* minigene immediately after the end of the transmembrane domain (residue 930), and fused an 11.2 kb SalI-SmaI *ced-1* fragment (the SalI site was from the vector polylinker) in-frame to GFP in vector pPD95.75. $P_{ced\text{-}1}$*ced-1Ex::gfp* was generated similarly, except that the SmaI site was added at the end of the CED-1 extracellular domain (amino acid 908). To generate $P_{ced\text{-}1}$*NLS-gfp*, we inserted the 5 kb $P_{ced\text{-}1}$ upstream to the SV40 nuclear localization sequence (NLS) tagged-*gfp* in vector pPD95.67. The 3.7 kb Form 1 *ced-1* cDNA was cloned into vectors containing the heat shock promoters *hsp16–2* and *hsp16–41* (Stringham et al., 1992), respectively, to generate two constructs that we refer to collectively as P_{hsp}*ced-1*. The *gfp* gene was fused to *ced-1* cDNA in-frame at codon 1052, creating P_{hsp}*ced-1::gfp*. The same *ced-1::gfp* fusion was cloned under the control of the $P_{col\text{-}10}$, $P_{lim\text{-}7}$, and $P_{egl\text{-}1}$ promoters to generate $P_{col\text{-}10}$*ced-1::gfp*, $P_{lim\text{-}7}$*ced-1::gfp*, and $P_{egl\text{-}1}$*ced-1::gfp*, respectively.

Site-Directed Mutagenesis

The single mutations N962A, Y965A, Y1019A, and double mutations N962A Y1019A, Y965A Y1019A were generated in *ced-1* cDNA using the QuikChange Site-Directed Mutagenesis Kit from Stratagene (La Jolla, CA) and introduced into $P_{ced\text{-}1}$*ced-1::gfp*.

Quantitation of Engulfment Defects

Engulfment defects were measured as the number of persistent cell corpses using Nomarski optics to view animals anesthetized with 30 mM NaN_3 and mounted on agar pads. For persistent cell corpses generated during embryogenesis, we counted corpses in the heads of young L1 larvae (with a gonadal primordium of four cells) or of mid-L3 larvae. In *ced-1* mutants, this number gradually decreased during larval development: in L1 animals there were an average of 27 corpses, whereas in mid-L3 animals there were an average of 18 corpses. For persistent cell corpses generated during larval development, we counted corpses in the posterior ventral cords of mid-L3 stage larvae, at which point all seven deaths in this region should have occurred at least 12 hr earlier (Sulston and Horvitz, 1977). To count persistent germ cell corpses, we scored one gonadal arm in each adult hermaphrodite two days after L4 molt.

Fluorescence Microscopy and Characterization of CED-1::GFP Clustering

To visualize GFP fluorescence, worms anesthetized with 2% 1-phenoxy-2-propanol and mounted on agar pads were observed using 40×, 63×, or 100× Plan-apochromat objectives at 512 nm emission. Images were captured as serial Z-sections of 1.0 μm interval by a Princeton Instruments Quantix cooled charge-coupled device camera on a Zeiss-Applied Precision DeltaVision restoration microscope, and deconvolved images were presented. We used the Data Inspection Program provided by the DeltaVision software to measure the intensity of the GFP signal. To quantitate the frequency of CED-1::GFP clustering around cell corpses, we counted the number of corpses labeled with a bright GFP-positive circle in the head of mid-L3 larvae, at which stage the GFP-positive corpses were the most prominent, or L1-stage larvae. Both full and partial GFP circles were counted as positives. To score the expression of $P_{ced\text{-}1}$*NLS-gfp* in persistent cell corpses, cell corpses were identified using Nomarski optics and then examined for the presence of a GFP signal inside.

Electron Microscopy

Mid-L3 stage larvae and adult hermaphrodites two days after L4 molt were sectioned as described by Gumienny et al. (1999) and photographed on a JEOL 1200CX electron microscope at 80 kv.

Acknowledgments

We thank R. Ellis and A. Gerber for identifying polymorphisms *nP42* and *nP45*; X. He and P. Sorger for giving us access to and help with the DeltaVision Deconvolution Microscope; A. Fire, V. Ambros, B. Conradt, and O. Hobert for plasmids; N. An for strain maintenance; E. Castor for determining DNA sequences; M. Alkema, E. Davison, X. He, B. Hersh, M. Krieger, and E. Speliotes for comments concerning this manuscript; and many members of the Horvitz laboratory for suggestions. H. R. H. is an Investigator of the Howard Hughes Medical Institute. Z. Z. was supported by Postdoctoral Fellowships from the Damon Runyon-Walter Winchell Foundation (DRG1343) and the Medical Foundation.

Received June 6, 2000; revised November 13, 2000.

References

Adachi, H., Tsujimoto, M., Arai, H., and Inoue, K. (1997). Expression cloning of a novel scavenger receptor from human endothelial cells. J. Biol. Chem. *272*, 31217–31220.

Bloom, L., and Horvitz, H.R. (1997). The *Caenorhabditis elegans* gene *unc-76* and its human homologs define a new gene family involved in axonal outgrowth and fasciculation. Proc. Natl. Acad. Sci. USA *94*, 3414–3419.

Brenner, S. (1974). The genetics of *Caenorhabditis elegans*. Genetics *77*, 71–94.

Campbell, I.D., and Bork, P. (1993). Epidermal growth factor-like modules. Curr. Opin. Struc. Biol. *3*, 385–392.

Chalfie, M., Tu, Y., Euskirchen, G., Ward, W.W., and Prasher, D.C. (1994). Green fluorescent protein as a marker for gene expression. Science *263*, 802–805.

Conradt, B., and Horvitz, H.R. (1999). The TRA-1A sex determination protein of *C. elegans* regulates sexually dimorphic cell deaths by repressing the *egl-1* cell death activator gene. Cell *98*, 317–327.

C. elegans Sequencing Consortium (1998). Genome sequence of the nematode *C. elegans*: a platform for investigating biology. Science *282*, 2012–2018.

Ellis, R.E., Jacobson, D.M., and Horvitz, H.R. (1991). Genes required for the engulfment of cell corpses during programmed cell death in *Caenorhabditis elegans*. Genetics *129*, 79–94.

Fadok, V.A., Bratton, D.L., Frasch, S.C., Warner, M.L., and Henson, P.M. (1998). The role of phosphatidylserine in recognition of apoptotic cells by phagocytes. Cell Death Diff. *5*, 551–562.

Fadok, V.A., Bratton, D.L., Rose, D.M., Pearson, A., Ezekewitz, R.A., and Henson, P.M. (2000). A receptor for phosphatidylserine-specific clearance of apoptotic cells. Nature *405*, 85–90.

Franc, N.C., Heitzler, P., Ezekowitz, R.A.B., and White, K. (1999). Requirement for Croquemort in phagocytosis of apoptotic cells in *Drosophila*. Science *284*, 1991–1994.

Giles, K.M., Hart, S.P., Haslett, C., Rossi, A.G., and Dransfield, I. (2000). An appetite for apoptotic cells? Controversies and challenges. Br. J. Haematol. *109*, 1–12.

Gumienny, T.L., Lambie, E., Hartwieg, E., Horvitz, H.R., and Hengartner, M.O. (1999). Genetic control of programmed cell death in the *Caenorhabditis elegans* hermaphrodite germline. Development *126*, 1011–1022.

Hall, D.H., Winfrey, V.P., Blaeuer, G., Hoffman, L.H., Furuta, T., Rose, K.L., Hobert, O., and Greenstein, D. (1999). Ultrastructural features of the adult hermaphrodite gonad of *Caenorhabditis elegans*: relations between the germ line and soma. Dev. Biol. *212*, 101–123.

Hamon, Y., Broccardo, C., Chambenoit, O., Luciani, M.F., Toti, F., Chaslin, S., Freyssinet, J.M., Devaux, P.F., McNeish, J., Marguet, D., and Chimini, G. (2000). ABC1 promotes engulfment of apoptotic cells and transbilayer redistribution of phosphatidylserine. Nat. Cell Biol. *2*, 399–406.

Hedgecock, E.M., Sulston, J.E., and Thomson, J.N. (1983). Mutations affecting programmed cell deaths in the nematode *Caenorhabditis elegans*. Science *220*, 1277–1279.

Kimble, J., Henderson, S., and Crittenden, S. (1998). Notch/LIN-12 signaling: transduction by regulated protein slicing. Trends Biochem. Sci. *23*, 353–357.

Krause, M., and Hirsh, D. (1987). A trans-spliced leader sequence on actin mRNA in *C. elegans*. Cell *49*, 753–761.

Krieger, M., and Herz, J. (1994). Structures and functions of multiligand lipoprotein receptors: macrophage scavenger receptors and LDL receptor-related protein (LRP). Annu. Rev. Biochem. *63*, 601–637.

Kwiatkowska, K., and Sobota, A. (1999). Signaling pathways in phagocytosis. Bioessays *21*, 422–431.

Kyte, J., and Doolittle, R.F. (1982). A simple method for displaying the hydropathic character of a protein. J. Mol. Biol. *157*, 105–132.

Liu, Q.A., and Hengartner, M.O. (1998). Candidate adaptor protein CED-6 promotes the engulfment of apoptotic cells in *C. elegans*. Cell *93*, 961–972.

Mello, C.C., Kramer, J.M., Stinchcomb, D., and Ambros, V. (1991). Efficient gene transfer in *C.elegans*: extrachromosomal maintenance and integration of transforming sequences. EMBO J. *10*, 3959–3970.

Metzstein, M.M., Stanfield, G.M., and Horvitz, H.R. (1998). Genetics of programmed cell death in *C. elegans*: past, present and future. Trends Genet. *14*, 410–416.

Murao, K., Terpstra, V., Green, S.R., Kondratenko, N., Steinberg, D.,

and Quehenberger, O. (1997). Characterization of CLA-1, a human homologue of rodent scavenger receptor BI, as a receptor for high density lipoprotein and apoptotic thymocytes. J. Biol. Chem. *272*, 17551–17557.

Nakayama, M., Nakajima, D., Nagase, T., Nomura, N., Seki, N., and Ohara, O. (1998). Identification of high-molecular-weight proteins with multiple EGF-like motifs by motif-trap screening. Genomics *51*, 27–34.

Oka, K., Sawamura, T., Kikuta, K., Itokawa, S., Kume, N., Kita, T., and Masaki, T. (1998). Lectin-like oxidized low-density lipoprotein receptor 1 mediates phagocytosis of aged/apoptotic cells in endothelial cells. Proc. Natl. Acad. Sci. USA *95*, 9535–9540.

Pawson, T., and Scott, J.D. (1997). Signaling through scaffold, anchoring, and adaptor proteins. Science *278*, 2075–2080.

Platt, N., Suzuki, H., Kurihara, Y., Kodama, T., and Gordon, S. (1996). Role for the class A macrophage scavenger receptor in the phagocytosis of apoptotic thymocytes *in vitro*. Proc. Natl. Acad. Sci. USA *93*, 12456–12460.

Platt, N., da Silva, R.P., and Gordon, S. (1998). Recognizing death: the phagocytosis of apoptotic cells. Trends Cell Biol. *8*, 365–372.

Reddien, P.W., and Horvitz, H.R. (2000). CED-2/CrkII and CED-10/Rac control phagocytosis and cell migration in *Caenorhabditis elegans*. Nat. Cell Biol. *2*, 131–136.

Ren, Y., Silverstein, R.L., Allen, J., and Savill, J. (1995). CD36 gene transfer confers capacity for phagocytosis of cells undergoing apoptosis. J. Exp. Med. *181*, 1857–1862.

Riddle, D.L., Blumenthal, T., Meyer, B.J., and Priess, J.R. (1997). *C. elegans* II (Plainview, NY: Cold Spring Harbor Laboratory Press).

Robertson, A.M.G., and Thomson, J.N. (1982). Morphology of programmed cell death in the ventral nerve cord of *Caenorhabditis elegans* larvae. J. Embryol. Exp. Morph. *67*, 89–100.

Sambrano, G.R., and Steinberg, D. (1995). Recognition of oxidatively damaged and apoptotic cells by an oxidized low density lipoprotein receptor on mouse peritoneal macrophages: role of membrane phosphatidylserine. Proc. Natl. Acad. Sci. USA *92*, 1396–1400.

Savill, J.S., Fadok, V., Henson, P., and Haslett, C. (1993). Phagocyte recognition of cells undergoing apoptosis. Immunol. Today *14*, 131–136.

Stringham, E.G., Dixon, D.K., Jones, D., and Candido, E.P. (1992). Temporal and spatial expression patterns of the small heat shock (hsp16) genes in transgenic *Caenorhabditis elegans*. Mol. Biol. Cell *3*, 221–233.

Stryer, L. (1988). Biochemistry, 3rd Edition (New York: W. H. Freeman and Company).

Sulston, J.E., and Horvitz, H.R. (1977). Post-embryonic cell lineages of the nematode, *Caenorhabditis elegans*. Dev. Biol. *56*, 110–156.

Sulston, J.E., Schierenberg, E., White, J.G., and Thomson, N. (1983). The embryonic cell lineage of the nematode *Caenorhabditis elegans*. Dev. Biol. *100*, 64–119.

Tait, J.F., and Smith, C. (1999). Phosphatidylserine receptors: role of CD36 in binding of anionic phospholipid vesicles to monocytic cells. J. Biol. Chem. *274*, 3048–3054.

Trommsdorff, M., Gotthardt, M., Hiesberger, T., Shelton, J., Stockinger, W., Nimpf, J., Hammer, R.E., Richardson, J.A., and Herz, J. (1999). Reeler/Disabled-like disruption of neuronal migration in knockout mice lacking the VLDL receptor and ApoE receptor *2*. Cell *97*, 689–701.

Van Aelst, L., and D'Souza-Schorey, C. (1997). Rho GTPases and signaling networks. Genes Dev. *11*, 2295–2322.

Vaux, D.L., and Korsmeyer, S.J. (1999). Cell death in development. Cell *96*, 245–254.

Weng, J., Mata, N.L., Azarian, S.M., Tzekov, R.T., Birch, D.G., and Travis, G.H. (1999). Insights into the function of Rim protein in photoreceptors and etiology of Stargardt's disease from the phenotype in *abcr* knockout mice. Cell *98*, 13–23.

Wu, Y., and Horvitz, H.R. (1998a). The *C. elegans* cell corpse engulfment gene *ced-7* encodes a protein similar to ABC transporters. Cell *93*, 951–960.

Wu, Y., and Horvitz, H.R. (1998b). *C. elegans* phagocytosis and cell-migration protein CED-5 is similar to human DOCK180. Nature *392*, 501–504.

Wyllie, A.H., Kerr, J.F.R., and Currie, A.R. (1980). Cell death: the significance of apoptosis. International Review of Cytology *68*, 251–306.

Zhou, S., and Cantley, L.C. (1995). Recognition and specificity in protein tyrosine kinase-mediated signalling. Trends Biochem. Sci. *20*, 470–475.

GenBank Accession Number

The GenBank accession number for ced-1 is AF332568.